of the NPP molecules in the sol-gel matrix. No crystallization of NPP molecules has been observed. The number density and the $\chi^{(2)}$ values are both considerably higher than that previously reported by Puccetti.[17]

In conclusion, we have achieved high second-order nonlinearity in a sol-gel-processed inorganic oxides:organic compound composite. The NLO active organic molecules have been aligned by an applied electric field. Both second harmonic generation and electrooptic modulation have been studied. Long-term stability of a bulk second-order susceptibility has been obtained.

Acknowledgment. Y.Z. thanks Drs. K. Wijekoon and M. Samoc and Mr. Y. P. Cui for helpful discussions. This research was supported by the Office of Innovative Science and Technology of the Strategic Defence Initiative Organization and the Air Force Office of Scientific Research, Directorate of Chemical and Atmospheric Sciences through Contract Nos. F49620-91-C-0053 (Photonics Research Laboratory, SUNY at Buffalo) and F49620-90-C-0052 (Laser Photonics Technology, Inc.).

Registry No. *N*-(4-nitrophenyl)-(*s*)-prolinol, 88422-19-9; silica, 7631-86-9; titanium dioxide, 13463-67-7.

(17) Puccetti, G.; Toussaere, E.; Ledoux, I.; Zyss, J. *Polym. Prepr. (Am. Chem. Soc., Div. Polym. Chem.)* **1991**, *32*, 61.

Silica-Pillared Derivatives of H^+-Magadiite, a Crystalline Hydrated Silica

James S. Dailey and Thomas J. Pinnavaia*

Department of Chemistry and Center for Fundamental Materials Research, Michigan State University, East Lansing, Michigan 48824

Received February 4, 1992. Revised Manuscript Received March 20, 1992

H^+-magadiite ($H_4Si_{14}O_{30}\cdot H_2O$), a hydrous lamellar silicic acid formed by proton ion exchange of Na^+-magadiite ($Na_{1.7}H_{1.9}Si_{14}O_{29.8}\cdot 7.7H_2O$), reacts with neat octylamine to form an octylamine/octylammonium-magadiite gel with a basal spacing (34 Å) corresponding to the presence of an intercalated bilayer of onium ions and amine molecules. Reaction of the swollen gel with neat tetraethylorthosilicate at TEOS:magadiite ratios in the range 54:1 to 154:1, followed by drying of the solid products in air, affords siloxane-intercalated derivatives with basal spacings of 23-28 Å. FTIR studies and analytical results indicate that TEOS intercalation occurs by displacement of octylamine. Also, TEM images show that the hydrolyses and condensation-polymerization of TEOS is topotactic. Calcination of the siloxane intercalates at 300 °C yields silica-pillared magadiites with basal spacings of 20.7-25.9 Å and *microporous* surface areas of 480-670 m^2/g. ^{29}Si MAS NMR results show that the overall Q^3 and Q^4 connectivity of SiO_4 units decreases from a ratio of 0.28 ± 0.02 for the air-dried siloxane derivatives to 0.19 ± 0.02 for the calcined silica pillared forms. Pristine H^+-magadiite exhibits a Q^3/Q^4 ratio of 0.28. However, the presence of Q^2 silicon environments in the silica-pillared products precludes the possibility of the pillars being isostructural with the magadiite layers.

Introduction

Pillared layered materials have attracted widespread interest over the past 10 years due in part of their catalytic and molecular sieving properties.[1-3] In an effort to broaden the diversity of pillared lamellar materials, we and several other groups of workers have been investigating the pillaring reactions of the hydrous sodium silicate Na^+-magadiite ($Na_2Si_{14}O_{29}\cdot 9H_2O$). Other examples of this unique family of silicates include, kenyaite ($Na_2Si_{20}O_{41}\cdot 10H_2O$), makatite ($Na_2Si_4O_9\cdot 5H_2O$), and kanemite ($NaHSi_2O_5\cdot 3H_2O$). All are naturally occurring minerals, many of which are found in lake beds at Lake Magadi, Kenya.[4] These compounds also can be conveniently prepared in the laboratory by hydrothermal synthesis.[5-7]

Intercalative ion-exchange reactions of Na^+-magadiite with robust cations is not a generally viable approach to synthesizing pillared derivatives, owing in part to the relatively high layer charge and limited swelling characteristics of the interlayers. For instance, our recent attempts to pillar Na^+-magadiite by ion exchange of cobalt sepulchrate, $[Co(sep)]^{3+}$, a metal cage complex noted for its exceptional stability in solution,[8] afforded instead a "stuffed", nonmicroporous intercalated derivative in which one-half of the metal centers were no longer complexed by the sepulchrate ligand.[9] Also, Fripiat and co-workers[10] have found that $KHSi_2O_5$, a related layer silicate, undergoes ion-exchange reaction with $Al_{13}O_4(OH)_{24}(H_2O)_{12}^{7+}$ cations, but the products are highly disordered.

The intercalation of grafted silyl groups in layered silicates appears to be a more promising approach to ordered

(1) Figueras, F. *Catal. Rev.* **1988**, *30*, 457.
(2) Vaughan, D. E. W. In *Perspectives in Molecular Sieve Science*; Flank, W. H., Whyte, T. E., Eds.; American Chemical Society: Washington, DC, 1988; p 308.
(3) *Pillared Layered Structures: Current Trends and Applications*; Mitchell, I. V., Ed.; Elsevier: New York, 1990.
(4) Eugster, H. P. *Science* **1967**, *157*, 1177.
(5) Fletcher, R. A.; Bibby, D. M. *Clays Clay Miner.* **1987**, *35*, 318.
(6) Beneke, K.; Lagaly, G. *Am. Miner.* **1983**, *68*, 818; **1977**, *62*, 763.
(7) Schwieger, W.; Heyer, W.; Wolf, F.; Bergk, K.-H. *Z. Anorg. Allg. Chem.* **1987**, *548*, 204.
(8) Creaser, I. I.; Geue, R. J.; Harrowfield, J. M.; Herlt, A. J.; Sargeson, A. M.; Snow, M. R.; Sprinborg, J. *J. Am. Chem. Soc.* **1982**, *104*, 6016.
(9) Dailey, J. S.; Pinnavaia, T. J. *J. Inclusion Phenom.*, in press.
(10) Deng, Z.; Lambert, J. F. H.; Fripiat, J. J. *Chem. Mater.* **1989**, *1*, 640.

0897-4756/92/2804-0855$03.00/0

pillared derivatives. Ruiz-Hitzky et al.[11] have found that H^+–magadiite preintercalated with dimethyl sulfoxide reacts with silane coupling agents to form intercalated derivatives with trimethylsilyl groups grafted to the gallery surface. Also, alkylammonium-exchanged forms of magadiite and kenyaite have been shown to react with trimethylchlorosilane to form silane-grafted derivatives with expanded basal spacing.[12]

More recently, Sprung et al.[13] reported that silsesquioxane aggregates formed by the hydrolysis of phenyltrichlorosilane can be intercalated in H^+–magadiite. Subsequent calcination of the reaction products at 350 °C afforded partially pillared derivatives with gallery heights of ~4.4 Å and surface areas in the range 100–200 m^2/g. A silica-pillared magadiite with a more substantial surface area has been reported by Landis and co-workers.[14] This latter group allowed tetraethylorthosilicate (TEOS) to react with an alkylammonium-exchanged form of magadiite and obtained a crystalline derivative containing an intercalated siloxane polymer. Upon calcining the siloxane derivative to remove organo groups, they formed a silica-pillared magadiite with high surface area (530 m^2/g).

We also have been investigating the reaction of TEOS and other metal alkoxides with layered silicates in an effort to form supergallery pillared derivatives. In a supergallery pillared clay, the gallery height is substantially larger than the thickness of the host layer.[15] Conventional metal oxide pillared clays typically exhibit gallery heights equal to or less than the thickness of the host layer. Hydrolysis and condensation polymerization of metal alkoxides in a layered silicic acid, such as magadiite, is a promising route to supergallery derivatives, because the gallery height generated by the siloxane polymer can be substantially larger than the 11.2-Å-thick host layers. In the present work we report the reaction of TEOS with octylammonium magadiite in the presence of excess amine and describe the silica-pillared magadiite derived from the intracrystal hydrolysis and condensation polymerization of TEOS.

Experimental Section

Na^+-Magadiite. Synthetic Na^+–magadiite was prepared by the reaction of NaOH and SiO_2 under hydrothermal conditions using methods analogous to those described by Fletcher and Bibby.[5] A suspension of Davisil 62 SiO_2 (12.0 g, 0.20 mol) in 60 mL of 1.1 M NaOH (0.067 mol) was allowed to digest without stirring at 150 °C for 46 h in a Teflon-lined stainless steel autoclave. The solid Na^+–magadiite reaction product was separated by centrifugation, washed twice with 200 mL of deionized H_2O in order to remove excess NaOH, and air-dried at 40 °C.

H^+-Magadiite. H^+–magadiite was prepared by titration of Na^+–magadiite with 0.1 N HCl by adaptation of the method of Lagaly et al.[16] A suspension composed of Na^+–magadiite (18.5 g) and 460 mL of deionized H_2O was titrated slowly with 0.1 N HCl. The pH of the Na^+–magadiite suspension, which was monitored with the aid of a pH meter, was lowered to 1.9 over 12 h and then maintained at this value for an additional 12 h. Solid H^+–magadiite was separated by centrifugation, washed with deionized H_2O until Cl^- free and then dried in air at 40 °C.

Octylammonium–Magadiite Gel. A reactive octylamine/octylammonium–magadiite gel was formed by allowing air-dried H^+–magadiite (0.5 g, 0.57 mmol) to react at room temperature with excess octylamine (2.0 g, 15 mmol). During octylamine addition, the H^+–magadiite absorbs the liquid amine, immediately forming a gray gelatinous mixture that will not flow. The resultant gel was used without further treatment for all reactions.

Silica-Intercalated Magadiites. Silica-intercalated derivatives of magadiite were prepared by the reaction of neat tetraethylorthosilicate, TEOS, with a gel composed of octylammonium–magadiite solvated by excess octylamine. To three 150-mL Erlenmeyer flasks, each containing the previously described gel formed from octylamine and H^+–magadiite (0.5 g, 0.57 mmol H^+–magadiite), were added three different aliquats of TEOS (6.3 g, 31 mmol; 10.3 g, 51 mmol; and 17.7 g, 87 mmol). The reaction flasks were covered, and the mixtures were stirred vigorously at room temperature for 24 h. The siloxane-intercalated reaction products were separated by centrifugation and dried from ethanol suspension in air at 40 °C. Calcined pillared derivatives were prepared by heating the air-dried solids in air at 360 °C for 4 h.

X-ray Powder Diffraction. Basal spacings were determined from the 00*l* X-ray reflections of oriented film samples using a Rigaku Rotaflex diffractometer equipped with Cu Kα radiation. Samples of Na^+–magadiite, H^+–magadiite, and the uncalcined TEOS/magadiite reaction products were prepared by depositing on a glass slide a suspension of the solids and allowing the suspension to air dry at 40 °C. Samples of the calcined silica-intercalated magadiite for X-ray diffraction analysis were prepared by heating the uncalcined TEOS/magadiite reaction products on glass microscope slides to 360 °C in air for 4 h. The basal spacing of octylamine/octylammonium–magadiite was obtained by smearing a thin film of the gel across a glass microscope slide and then recording the diffraction pattern of the wet sample.

^{29}Si MAS NMR. These experiments were performed on a Varian 400 VXR solid-state NMR spectrometer operated at 79.5 MHz. A Bruker multinuclear MAS probe equipped with zirconia rotors was used for all measurements. The ^{29}Si relaxation times for Na^+–magadiite, H^+–magadiite, and the uncalcined and calcined TEOS/magadiite reaction products were determined by the inversion recovery method. ^{29}Si MAS spectra were obtained using 4.6-μs 90° pulse widths. A total of 12 scans were accumulated for each sample. The spinning rate was 5 kHz. Delay times approximately 5 times as large as T_1 were used in order to obtain quantitative integral intensities. Cross-polarization experiments were carried out with delay times of 10 s and contact times of 1000 ms.

Surface Area Measurements. Nitrogen adsorption/desorption isotherms were determined on a Quantachrome Autosorb Sorptometer at liquid N_2 temperature using ultrahigh-purity N_2 and He as adsorbate and carrier gases, respectively. All samples were outgassed at 150 °C under vacuum for 12 h. Surface areas were determined using the BET equation and the *t*-plot method.[17]

Infrared Spectroscopy. Fourier transform infrared spectra were obtained on an IBM IR44 spectrometer using the KBr pressed pellet technique.

Thermal Analysis. Thermogravimetric analyses were performed using a Cahn TG System 121 thermogravimetric analyzer. All samples were heated to 1000 °C at a heating rate of 5 °C/min.

Results and Discussion

Na^+- and H^+–Magadiite. The basic hydrolysis of silica gel at 150 °C according to the method of Fletcher and Bibby[5] produced well-crystallized Na^+–magadiite. The X-ray diffraction pattern of a partially oriented film of the air-dried product, shown in Figure 1A, exhibited several 00*l* reflections corresponding to a basal spacing of 15.6 Å. Despite our efforts to produce well-oriented film samples for the diffraction experiments, several *hkl* reflections with $h \neq k \neq 0$ were observed due to the rosette-like morphology of the aggregated platelets. The peak positions for this synthetic product agree closely with values reported previously[18,19] for synthetic and natural magadiite.

(11) Ruiz-Hitzky, E.; Rojo, J. M.; Lagaly, G. *Colloid Polym. Sci.* **1985**, *263*, 1025.
(12) Yanagisawa, T.; Kuroda, K.; Kato, C. *React. Solids* **1988**, *5*, 167.
(13) Sprung, R.; Davis, M. E.; Kauffman, J. S.; Dybowski, C. *Ind. Eng. Chem. Res.* **1990**, *29*, 213.
(14) (a) Landis, M. E.; Aufdembrink, B. A.; Chu, P.; Johnson, I. D.; Kirker, G. W.; Rubin, M. K. *J. Am. Chem. Soc.* **1991**, *113*, 3189. (b) Landis, M. E.; Chu, P.; Johnson, I. D.; Kirker, G. W.; Rubin, M. K. U.S. Patent 4,859,648, 1989.
(15) Moini, A.; Pinnavaia, T. *J. Solid State Ionics* **1988**, *26*, 119.
(16) Lagaly, G.; Beneke, K.; Weiss, A. *Am. Miner.* **1975**, *60*, 650.
(17) Gregg, S. J.; Sing, K. S. W. *Adsorption, Surface Area and Porosity*, 2nd ed.; Academic Press: London, 1982.

Table I. Compositions of Synthetic and Natural Magadiite Samples

sample	wt %				atomic ratios		
	Na_2O	SiO_2	H_2O	Total	Na	Si	H_2O
Na^+–magadiite, synth (unwashed, this work)	6.58 (1.00)[a]	75.8 (11.9)	15.5 (8.11)	97.88	2.35	14	10.9
Na^+–magadiite, synth (washed, this work)	4.98 (1.00)	80.2 (16.6)	14.6 (10.0)	99.78	1.69	14	8.5
Na^+–magadiite, synth (Lagaly et al.[21])	5.58 (1.00)	74.9 (13.4)	18.2 (3.26)	98.68	2.02	14	11.3
Na^+–magadiite, natural (McAtee et al.[22])	5.60 (1.00)	77.4 (13.8)	15.2 (2.71)	98.2	2.13	14	9.2
Na^+–magadiite, synth (Garces et al.[19])	6.56 (1.00)	84.8 (12.9)	7.8 (1.19)	99.16	2.09	14	4.29
Na^+–magadiite, synth (Garces et al.[19])	6.31 (1.00)	87.0 (14.2)	8.1 (4.42)	101.4	1.96	14	4.35
H^+–magadiite, synth (this work)	<0.01	93.9	6.1	100.0	0	14	2.0

[a] Values in parentheses are mole ratios relative to Na_2O.

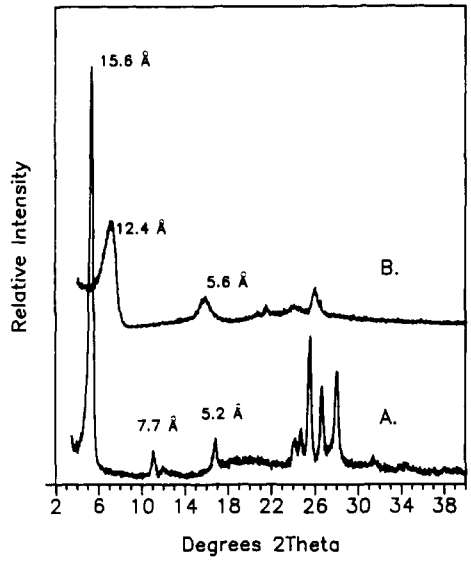

Figure 1. X-ray diffraction patterns for film samples of (A) Na^+–magadiite, and (B) H^+–magadiite.

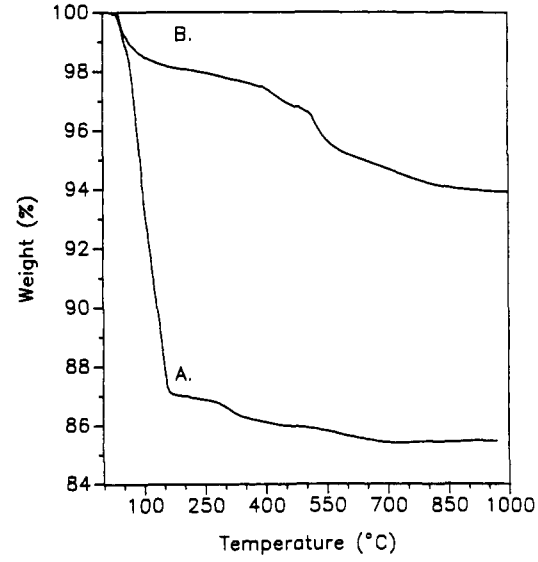

Figure 2. Thermogravimetric analysis curves obtained under flowing argon for (A) Na^+–magadiite, and (B) H^+–magadiite.

The slow titration of Na^+–magadiite with 0.1 N HCl resulted in the exchange of sodium ions for protons in the layer structure. The X-ray diffraction pattern of an air-dried H^+–magadiite film, shown in Figure 1B, exhibited 00*l* reflections corresponding to a basal spacing of 12.4 Å, in agreement with earlier work.[20] This decrease in basal spacing relative to the 15.6-Å sodium form indicated a loss of interlayer H_2O upon replacement of Na^+ by H^+. Also, the general broadening of the diffraction peaks indicated that greater stacking disorder occurred upon proton exchange.

The chemical composition of the Na^+–magadiite prepared in this work was obtained by combining the results of thermogravimetric analyses and chemical analyses. As shown by the thermogravimetric curve in Figure 2A, air-dried Na^+–magadiite that has been well washed with water to remove excess NaOH loses 13% of its total weight as water below 200 °C. An additional 1.6% by weight is lost between 200 and 1000 °C. The weight loss above 200 °C is assigned to the dehydroxylation of SiOH groups. By combining the Na_2O content (4.98%) and weight loss, we obtained an empirical composition for synthetic Na^+–magadiite of $Na_{1.7}Si_{14}O_{27.9}(OH)_{1.9}\cdot 7.6H_2O$. As shown by the data in Table I, our composition for Na^+ magadiite compares favorably with the approximate composition of $Na_2Si_{14}O_{29}\cdot 9H_2O$ supported by the earlier work of Lagaly et al.,[21] Garces et al.,[19] and McAtee et al.[22] We find that the sodium content of synthetic Na^+–magadiite depends in part on the extent to which the product is washed with water. Washing with water initially removes excess NaOH. However, repeated washing leaches Na^+ cations from the interlayer via hydrolysis. Thus, we attribute the relatively low sodium content of our washed product, 1.7 Na^+/14 Si, to hydrolysis caused by extensive washing. The variation in water content for the various Na^+–magadiite samples shown in Table I is presumably due to differences in drying conditions.

Thermal analysis of H^+–magadiite, as shown by the curve in Figure 2B, indicated an initial weight loss below 300 °C of 2.1% due to the desorption of H_2O. The 4.0% weight loss above 300 °C was attributed to the elimination of OH groups from the structure. The water loss together with the virtual absence of sodium, is in agreement with an approximate unit cell composition of $H_4Si_{14}O_{30}\cdot H_2O$. This formula compares favorably with the compositions such as $H_2Si_{14}O_{29}\cdot 5H_2O$ reported by other workers.[13,16]

Octylamine/Octylammonium–Magadiite. Lagaly and co-workers[16] have previously reported that H^+–magadiite intercalated by dimethyl sulfoxide (DMSO) reacts with alkylamines to form ordered bilayers of alkylammonium and alkylamine molecules between the silicate layers. This property of solvated H^+–magadiite is analogous to the ordering that occurs in the galleries of *n*-alkylammonium montmorillonites swollen by *n*-alkyl alcohols or amines.[23] We find that our air-dried H^+–magadiite reacts directly with octylamine without the need for preintercalation by DMSO. The X-ray diffraction pattern shown in Figure 3A for the air-dried octylammonium–

(18) Brindley, G. W. *Am. Miner.* **1969**, *54*, 1583.
(19) Garces, J. M.; Rocke, S. C.; Crowder, C. E.; Hasha, D. L. *Clays Clay Miner.* **1988**, *36*, 409.
(20) Rojo, J. M.; Ruiz-Hitzky, E.; Sanz, J. *Inorg. Chem.* **1988**, *27*, 2785.
(21) Lagaly, G.; Beneke, K.; Weiss, A. *Am. Miner.* **1975**, *60*, 642.
(22) McAtee, J. L.; House, R.; Eugster, H. P. *Am. Miner.* **1968**, *53*, 2061.
(23) Weiss, A. *Angew. Chem., Int. Ed. Engl.* **1963**, *2*, 134.

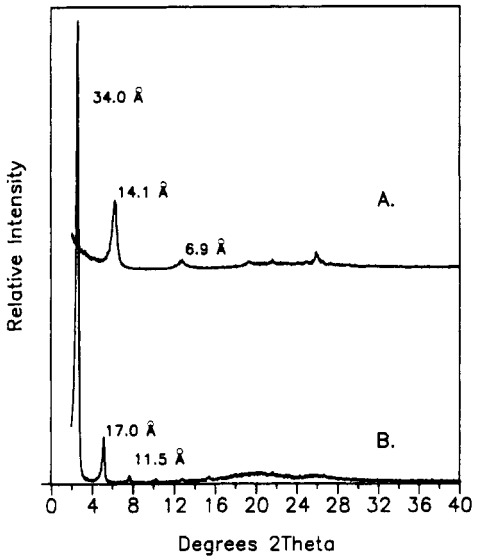

Figure 3. X-ray diffraction patterns for film samples of octylammonium–magadiite (A) sample air-dried at 25 °C and (B) solvated by excess octylamine.

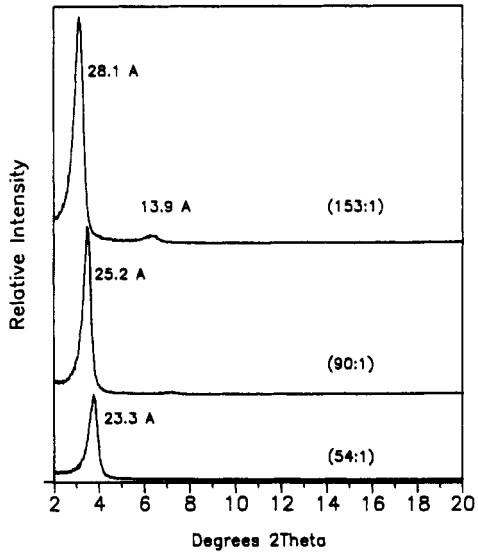

Figure 4. X-ray diffraction patterns for film samples of the uncalcined TEOS/magadiite reaction products that resulted from treatment of octylamine solvated octylammonium–magadiite with tetraethylorthosilicate. TEOS/magadiite mole ratios were 54:1, 90:1, and 153:1.

magadiite is indicative of a 14.1-Å basal spacing or a 2.9-Å gallery height. Thus, the octylammonium cations are intercalated in the air-dried sample with the chains orientated parallel to the silicate layer. However, the X-ray diffraction pattern of octylammonium–magadiite changes dramatically upon solvation by excess octylamine, as shown in Figure 3B. The gallery height for the amine-solvated gel was 22.8 Å, which indicates the formation of bilayers of octylammonium ions and octylamine molecules between the silicate layers.

Reactions with TEOS. The reactions of octylamine/octylammonium–magadiite with neat tetraethylorthosilicate (TEOS), followed by drying of the solid products in air, afford siloxane-intercalated derivatives with well-ordered basal spacings. Figure 4 illustrates the X-ray diffraction patterns for the air-dried intercalates isolated from reaction mixtures containing 54, 90, and 153 mol of TEOS/mol of magadiite. These products exhibit reflections corresponding to basal spacings of 23.3, 25.2, and 28.1 Å, respectively. Since the layer thickness of

Table II. Basal Spacing and Gallery Heights of Magadiite Reaction Precursors and TEOS Reaction Products

sample	basal spacing, Å	gallery ht, Å
Na^+–magadiite	15.6	4.4
H^+–magadiite	12.4	1.2
$C_8H_{17}NH_3^+$–magadiite (air dried)	14.1	2.9
$C_8H_{17}NH_3^+$–magadiite (amine solvated)	34.0	22.8
TEOS/magadiite (54:1)	23.3	12.1
TEOS/magadiite (90:1)	25.2	14.0
TEOS/magadiite (153:1)	28.1	16.9
TEOS/magadiite (54:1, calcined 360 °C)	20.7	9.5
TEOS/magadiite (90:1, calcined 360 °C)	22.4	11.2
TEOS/magadiite (153:1, calcined 360 °C)	25.9	14.7

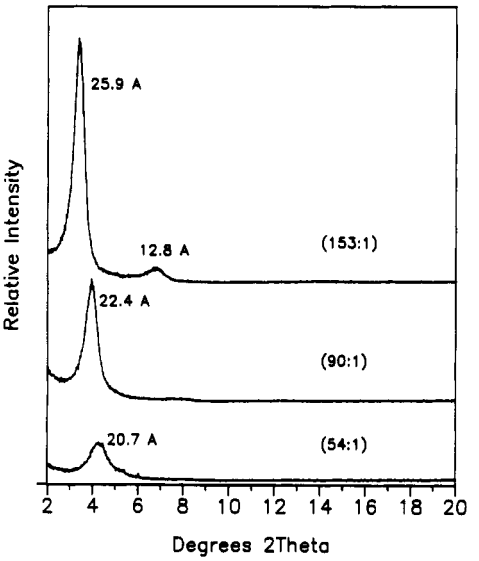

Figure 5. X-ray diffraction patterns for film samples of TEOS/magadiite reaction products after calcination. Calcined in air at 360 °C for 4 h.

magadiite is 11.2 Å, the corresponding gallery heights are 12.1, 14.0, and 16.9 Å, respectively. These gallery heights for the siloxane intercalates are ~5–10 Å smaller than the initial gallery height of 22.8 Å observed for the octylamine/octylammonium–magadiite precursor gel.

Calcination of the siloxane intercalates at 360 °C to remove organic components yields silica intercalated products with basal spacings only 2–3 Å smaller than the siloxane precursors (Figure 5). Table II summerizes the *d* spacings and gallery heights for the starting materials along with those for the air-dried and calcined TEOS/magadiite reaction products.

The compositions of the products obtained by reaction of octylamine/octylammonium–magadiite with TEOS were derived from TGA and C, H, N, chemical analyses. All nitrogen was assumed to be due to the presence of octylammonium cation and octylamine. Carbon in excess of the amount expected for octylammonium/octylamine was attributed to the presence of residual alkoxide associated with polymerized siloxane. The results are presented in Table III, along with the compositions of H^+–magadiite and air-dried octylammonium–magadiite. It is noteworthy that the percentage of octylammonium/octylamine present in the uncalcined reaction products decreases as the amount of TEOS used in the reaction increases, suggesting that the neutral amine is replaced to a larger extent as the amount of TEOS present in the reaction mixture increases. All three reaction products contain some residual ethoxide. Apparently, some $SiOC_2H_5$ linkages are not hydrolyzed when the products are dried in air. The amine content of the samples is similar to the amount present in air-dried

Table III. Compositions (wt %) of Magadiite Reaction Products

sample	SiO_2[a]	$C_8H_{17}NH_2$[b]	C_2H_5–O[c]	H_2O[d]	total
H^+-magadiite	93.9			6.1	100
$C_8H_{17}NH_3^+$-magadiite[e] (air dried)	84.4	11.1		5.0	100
TEOS/magadiite (54:1)[f]	79.0	13.5	2.4	2.9	97.8
TEOS/magadiite (90:1)	77.7	12.4	3.8	4.8	98.7
TEOS/magadiite (153:1)	80.4	10.4	3.3	4.5	98.6

[a] Based on weight retained after heating to 1000 °C. [b] Values obtained by nitrogen analyses. [c] Values based on excess carbon/hydrogen. [d] Obtained by weight loss below 200 °C. [e] This air-dried product contains only a 0.9 mol of amine/mol of magadiite and is not representative of the composition of the octylamine/octylammonium magadiite gel used as TEOS reaction precursor. [f] Reaction mixture stoichiometry in mol of TEOS/mol of magadiite.

Table IV. Surface Area Analyses (m^2/g) for Calcined TEOS–Octylamine/Octyalmmonium–Magadiite Reaction Products[a]

sample	S_{BET}	S_{total}	S_{mic}	S
H^+–magadiite	45	45	0	45
TEOS/magadiite (54:1)	620	635	590	45
TEOS/magadiite (90:1)	680	705	670	35
TEOS/magadiite (153:1)	520	525	480	45

[a] S_{BET} is the N_2 BET surface area; S_{total}, S_{mic}, and S are the total, microporous, and nonmicroporous surface areas, respectively, obtained from *t*-plots of the nitrogen adsorption data.

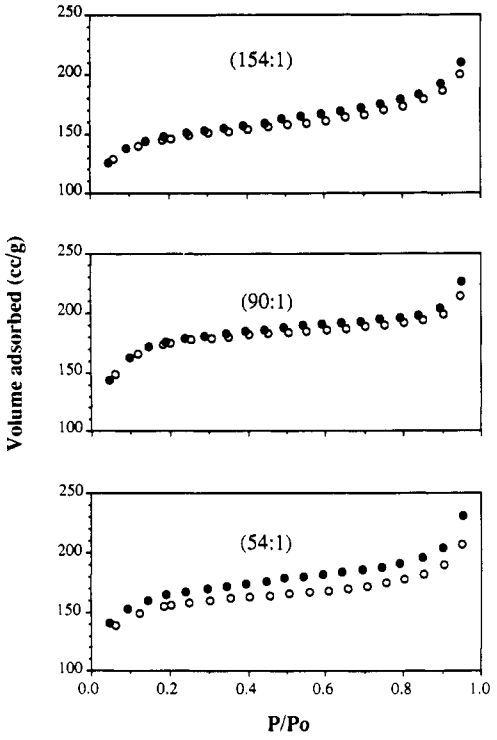

Figure 6. Nitrogen adsorption/desorption isotherms for the calcined TEOS/magadiite reaction products produced with a ratio of 54:1, 90:1, and 153:1 mol of TEOS/mol of magadiite.

octylammonium–magadiite (0.86 mol/Si_{14} unit), indicating that the electrostatically bound octylammonium cations are retained upon reaction with TEOS and that most of the neutral amine molecules are displaced by the silicon alkoxide.

The nitrogen adsorption/desorption isotherms shown in Figure 6 were obtained for calcined (360 °C) TEOS/magadiite reaction products. Surface area were obtained by fitting the adsorption data below $P/P_0 = 0.1$ to the BET equation.[17] The BET surface areas for H^+–magadiite and the calcined TEOS/magadiite reaction products are listed in Table IV. Included in the table are the total surface

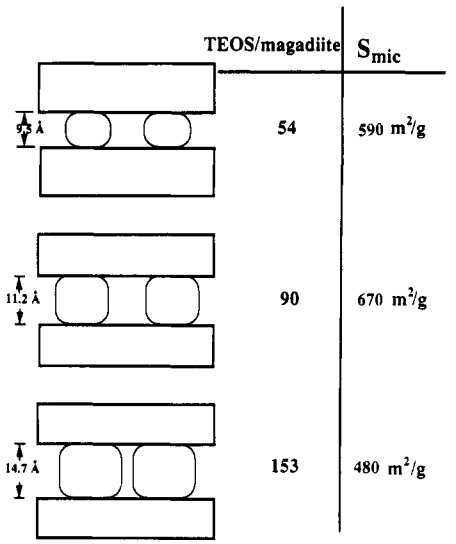

Figure 7. Schematic representation for the variation of pillar size with the change in reaction stoichiometry.

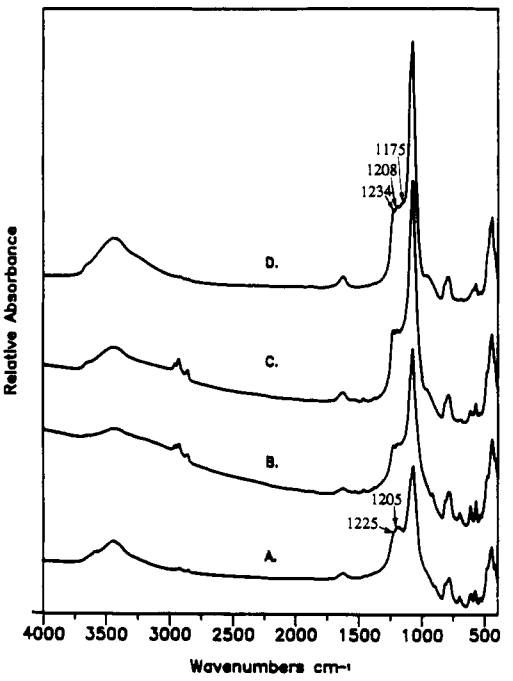

Figure 8. Infrared spectra (KBr disks) for (A) H^+–magadiite, (B) air-dried octylammonium–magadiite, (C) 90:1 TEOS/magadiite reaction product air dried, and (D) 90:1 TEOS/magadiite reaction product after calcining at 360 °C.

areas (S_{total}), the microporous surface areas (S_{mic}), and the nonmicroporous surface areas (S) obtained by using the *t*-plot method[17] and assuming the presence of parallel pores.

H^+–magadiite has a total surface area of 45 m^2/g due exclusively to adsorption at nonporous external surfaces. The calcined products obtained from the reaction of TEOS with octylamine/octylammonium magadiite exhibited dramatically larger surface areas between 520–680 m^2/g, depending on the amount of TEOS used in the reaction. Most of the total surface area is due to the presence of micropores <20 Å in diameter. The relationship between the microporous surface area, (cf. Table IV) and the gallery height (cf Table II) indicates a dependence of microporosity on TEOS reaction stoichiometry. Figure 7 schematically illustrates this dependence. An optimum microporous surface area of 670 m^2/g is obtained at an intermediate gallery height of 11.2 Å (mol of TEOS/mol of

magadiite = 90:1). This can be explained by a symmetrical increase in pillar size as the gallery height increases. Thus, as the pillar size increases the lateral spacing between pillars will decrease. An intermediate value of the gallery height would yield an optimum porosity when the best compromise exists between pillar height and lateral pillar spacing.

FTIR Spectra. The infrared spectra of calcined and uncalcined reaction products formed at a 90:1 TEOS/magadiite ratio are compared in Figure 8 with the spectra for octylammonium–magadiite and H^+–magadiite. The calcined product and H^+–magadiite exhibit similar spectra between 4000 and 400 cm^{-1}. Analogous spectra have been reported for Na^+–magadiite.[19] The broad overlaping bands centered at 3445 cm^{-1} are attributed to the OH group stretching frequencies of the silanol moieties and water associated with the silicate surface. The band centered at 1632 cm^{-1} is due to the bending frequency of H_2O. The remaining bands from 1500 to 400 cm^{-1} arise from the stretching and bending frequencies of the SiO_4 units that make up the magadiite layer. In the case of Na^+–magadiite, Garces et al.[19] have attributed a band at 1237 cm^{-1} to five-membered ring blocks of SiO_4 tetrahedra. In addition, the bands at 1210 and 1175 cm^{-1} were attributed to five-, six-, and four-membered ring block structures similar to those found in the zeolites epistilbite and dachiardite.[19] These same spectral features are clearly present for the calcined 90:1 TEOS:magadiite product and H^+–magadiite. These results indicate that there is retention of the magadiite layer structure upon pillaring by silica.

The infrared spectrum of the uncalcined 90:1 TEOS: magadiite reaction product exhibits IR bands which match closely those for the octylammonium–magadiite (cf. Figure 8, spectra B and C). In addition to the bands characteristic of the magadiite layers, weak bands at 2962, 2929, 2873, and 2859 cm^{-1} are observed for the C–H asymmetric and C–H symmetric stretching frequencies of the intercalated octylammonium cation. Weak broad bands centered at 1537 cm^{-1} are attributed to the NH_3^+ deformation (bending) frequency. A weak absorption at 1469 cm^{-1} results from the C–H asymmetric bending of the alkyl chain. This result is consistent with the analytical data, indicating the presence of electrostatically bound octylammonium ion in the uncalcined TEOS reaction product.

A weak band at 923 cm^{-1} in octylammonium–magadiite is assigned to the Si–O stretch of SiOH groups. A similar band is found in freshly precipitated silica gels near 950 cm^{-1} [24] and in hydrolyzed polysiloxane polymers near 890 cm^{-1}.[25] The band shifts from 923 to 958 cm^{-1} upon reaction with TEOS. This shift may be due in part to overlapping Si–O stretching frequency of the intercalated polysiloxane, which occurs near 1104 cm^{-1}.[26] After calcination of the 90:1 TEOS:magadiite reaction product at 360 °C, the bands characteristic of the octylammonium cation (2900, 1460, 1539 cm^{-1} virtually disappear. In addition, the Si–OH stretch near 958 cm^{-1} in the uncalcined material shifts to 965 cm^{-1} after calcination, indicating the formation of Si–O–Si linkages.[24]

^{29}Si MAS NMR. Figure 9 compares the spectra for the air-dried siloxane derivatives of magadiite with those for H^+– and Na^+–magadiite. The ^{29}Si MAS NMR spectra for the calcined (360 °C) silica-pillared magadiites are presented in Figure 10. All of these materials exhibit a Q^3 RO $Si(OSi)_3$ (R = H, Na) resonance near 100 ppm and multiple Q^4 Si $(OSi)_4$ lines in the range −110 to −114 ppm. A weak Q^2 $(HO)_2Si(OSi)_2$ resonance also is observed at 92.2 ppm for the calcined 90:1 TEOS/magadiite reaction product.

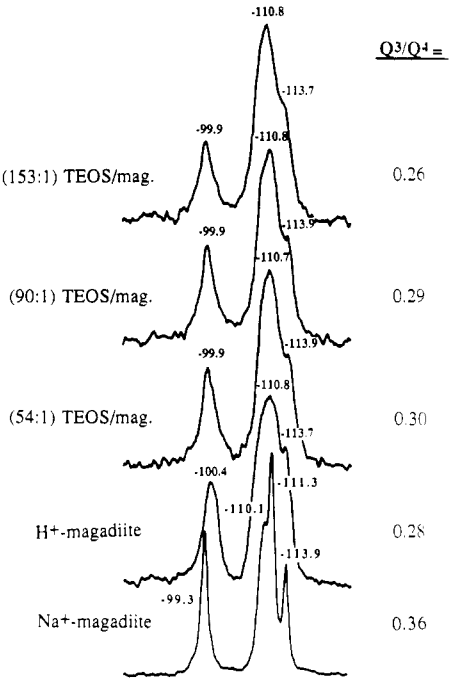

Figure 9. ^{29}Si MAS NMR spectra of Na^+–magadiite, H^+–magadiite, and uncalcined TEOS/magadiite reaction products.

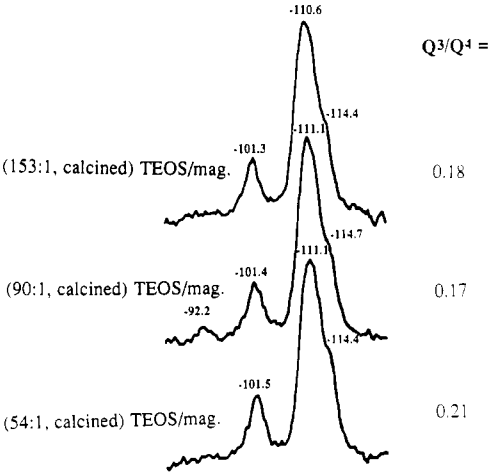

Figure 10. ^{29}Si MAS NMR spectra of calcined TEOS/magadiite reaction products.

The ^{29}Si chemical shifts and relative Q^3/Q^4 intensities for Na^+– and H^+– magadiite are in agreement with previously reported spectra.[9,27,28,29,30] H^+–magadiite exhibits spin–lattice relaxations times (T_1) of 95 s for both the Q^3 and the Q^4 silicon environments. In contrast, the Na^+ derivative gave substantially different T_1 values of 160 and 280 s for the Q^3 an dQ^4 environments, respectively. The calcined silica pillared products also exhibited T_1 relaxation times that were shorter for the Q^3 environments (44 ± 5

(24) Hino, M.; Sato, T. *Bull. Chem. Soc. Jpn.* **1971**, *44*, 33.
(25) Ishida, H. In *Adhesion Aspects of Polymeric Coatings*; Mittal, K. L., Ed.; Plenum: New York, 1983; p 45.
(26) Chaing, C. H.; Ishiada, H.; Koenig, J. L. *J. Colloid Interface Sci.* **1980**, *74*, 396.
(27) Pinnavaia, T. J.; Johnson, I. D.; Lipsicas, M. *J. Solid State Chem.* **1986**, *63*, 118.
(28) Schlzen, G.; Beneke, K.; Lagaly, G. *Z. Anorg. Allg. Chem.* **1991**, *597*, 183.
(29) Barron, P. F.; Slade, P.; Frost, R. L. *J. Phys. Chem.* **1985**, *89*, 3305.
(30) Lagaly, G. *Adv. Colloid Interface Sci.* **1979**, *11*, 105.

Table V. ^{29}Si MAS NMR Chemical Shift Values and Q^3/Q^4 Ratios for H⁺-Magadiite and the TEOS/Magadiite Reaction Products

sample	chemical shift, ppm Q^2	Q^3	Q^4	Q^3/Q^4 Ratio
H⁺-magadiite		-100.4	-110.8, -113.7	0.28
TEOS/magadiite (54:1,[a] air dried)		-99.9	-110.7, -113.9	0.30
TEOS/magadiite (90:1, air dried)		-99.9	-110.8, -113.9	0.29
TEOS/magadiite (153:1, air dried)		-99.9	-110.8, -113.7	0.26
TEOS/magadiite (54:1, calcined at 360 °C)		-101.5	-111.1, -114.4	0.21
TEOS/magadiite (90:1, calcined at 360 °C)	-92.2	-101.4	-111.1, -114.7	0.18
TEOS/magadiite (153:1, calcined at 360 °C)		-101.3	-110.6, -114.4	0.17
	CP-MAS			
TEOS/magadiite (54:1)		-101.6	-113.7	
TEOS/magadiite (90:1)		-101.6	-113.2	
TEOS/magadiite (153:1)	-90.5	-101.2	-112.7	
TEOS/magadiite (54:1, calcined at 360 °C)	-90.8	-101.4	-111.9	
TEOS/magadiite (90:1, calcined at 360 °C)	-91.0	-101.2	-111.7	
TEOS/magadiite (153:1 calcined at 360 °C)	-91.3	-101.6	-112.9	

[a] TEOS:H⁺-magadiite reaction stoichiometry (mole:mole).

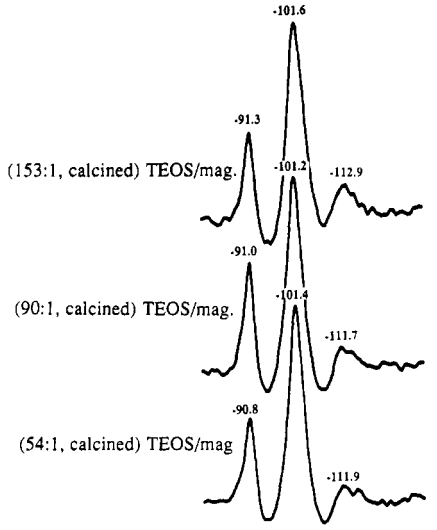

Figure 11. CP ^{29}Si MAS NMR spectra of calcined TEOS/magadiite reaction products.

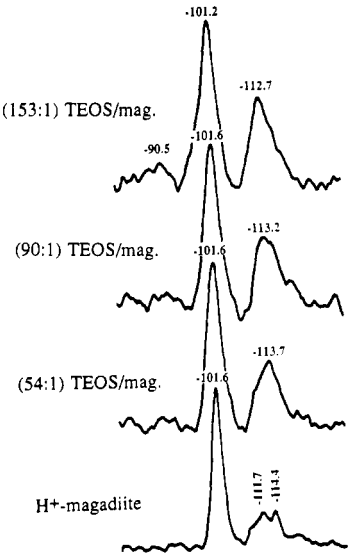

Figure 12. CP^{29}Si MAS NMR spectra of H⁺-magadiite and uncalcined TEOS/magadiite reaction products.

s) than the Q^4 sites (141 ± 11 s), depending in part on the state of hydration. ^{29}Si–^{1}H dipolar relaxation mechanisms may contribute to shorter relaxation times for the Q^3 environments. The importance of ^{29}Si–^{1}H dipolar relaxation via the OH dipoles of water molecules has been demonstrated for other layered silicate minerals.[29]

As shown by the data in Table V, the Q^3 and Q^4 chemical shifts for H⁺-magadiite and the calcined and air-dried TEOS/magadiite reaction products are remarkably similar. Analogous resonances occur in the spectrum of Na⁺-magadiite, except that the lines widths are narrower and three resonances are resolved in the Q^4 region (cf. Figure 9). The Q^3/Q^4 intensity ratios are especially striking feature of the ^{29}Si MAS NMR spectra for the air-dried TEOS/magadiite reaction products. The Q^3/Q^4 value of 0.28 ± 0.02 for the magadiite reaction products (cf. Table V and Figure 9) is independent of the TEOS/magadiite reaction stoichiometry and equals, within experimental uncertainty, the value observed for air-dried H⁺-magadiite. That is, the connectivity of SiO_4 tetrahedra in the siloxane pillars closely mimics the connectivity of the magadiite layers. This result, together with the molecular regularity of the pillars (as revealed by the basal spacings), suggests that the polymerization process is topochemical, if not topotactic. Calcination at 360 °C causes the Q^3/Q^4 ratio to decrease from a value of 0.28 ± 0.02 to 0.19 ± 0.02, presumably due to condensation of some Q^3 environments in both the pillars and the layers.

Proton cross-polarized ^{29}Si MAS spectra for the calcined silica-pillared magadites shown in Figure 11 reveal a resonance near -91 ppm, in addition to an enhanced Q^3 resonance near -101.5 ppm. The resonance at -91 ppm is assigned to a Q^2 $(HO)_2Si(OSi)_2$ environment which typically is too low in concentration to be observed in the normal spectra. The cross polarization spectra of the air-dried siloxane/magadiite precursors, shown in Figure 12, all exhibit a Q^3 resonance near -101.6 ppm and Q^4 resonances at approximately -113 ppm. In each case, the Q^3 resonance has been enhanced, confirming the presence of silanol groups. These $Q^3(HOSi(OSi)_3$ groups may be associated with either the layer or the siloxane pillar. The siloxane product obtained at a TEOS:magadiite reaction stoichiometry of 153:1 exhibits a very weak Q^2 resonance near -90.5 ppm. The low abundance of Q^2 environments in the CP spectra of the air-dried derivatives indicates the Q^2 environments are present as ethoxide rather than hydroxyl groups. Calcination results in combustion of the ethoxide groups and the formation of SiOH groups. Finally, it is noteworthy that proton cross polarization of ^{29}Si nuclei in H⁺-magadiite (cf. Figure 12) results in the enhancement of the Q^3 resonance centered at -101.6 ppm,

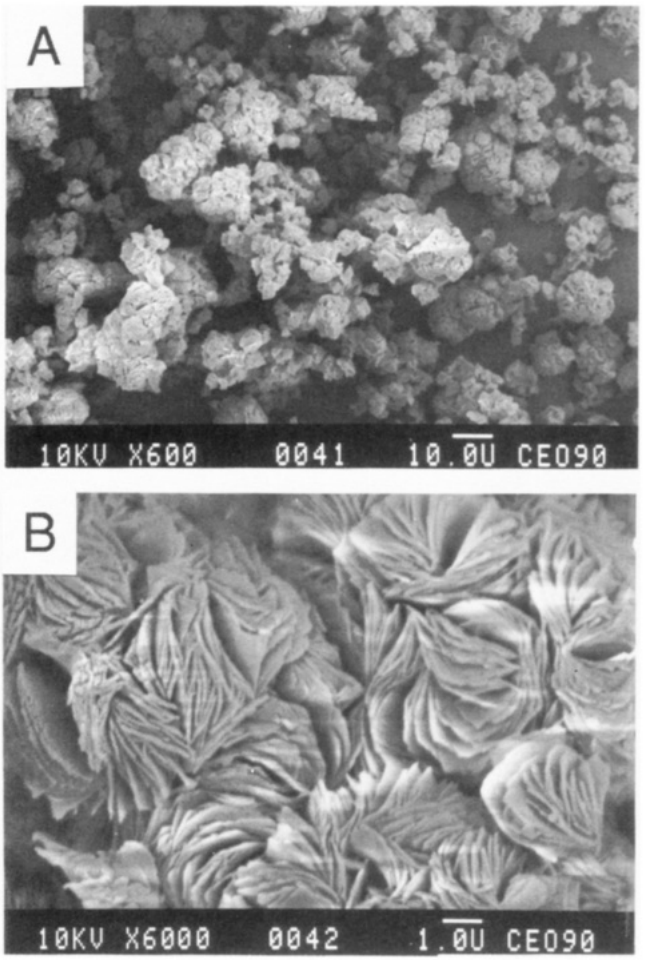

Figure 13. Scanning electron micrographs of H^+–magadiite at (A) ×6000 and (B) ×600 magnification.

thus confirming this assignment.

Morphology. Na^+–magadiite is known to adopt a particle morphology composed of silicate layers intergrown to form spherical nodules resembling rosettes.[19] The proton exchange form also exhibits this characteristic particle morphology,[30] as shown by the micrographs in Figures 13. Scanning electron micrographs of octylammonium–magadiite indicate that the rosette morphology is lost upon conversion of H^+ to onium ion by reaction with the free amine (Figure 14A). It appears that the expansion and contraction caused by octylamine intercalation followed by air drying results in a breakup of the spherical nodules and the concomitant parallel arrangement of the platelets. Scanning electron micrographs of the air-dried and calcined TEOS/magadiite products, shown in Figure 14B,C, respectively, exhibit the same platy morphology as octylammonium–magadiite. The similarity between the morphology of octylammonium–magadiite and the calcined and uncalcined TEOS/magadiite reaction products indicated that intercalation of TEOS occurs in a topotactic fashion.

Mechanism. The reaction of H^+–magadiite with octylamine forms an intercalate with a bilayer of octylammonium cations and neutral octylamine molecules between the layers, as illustrated schematically in Figure 15. The subsequent reaction of this intercalated derivative with tetraethylorthosilicate results in the replacement of the neutral octylamine with TEOS. As the TEOS replaces the octylamine, the SiOH groups of the host layer react with the siloxane groups to form siloxane bonds and EtOH. Further hydrolysis of the intercalated siloxane occurs during the air-drying process. Calcination of the siloxane

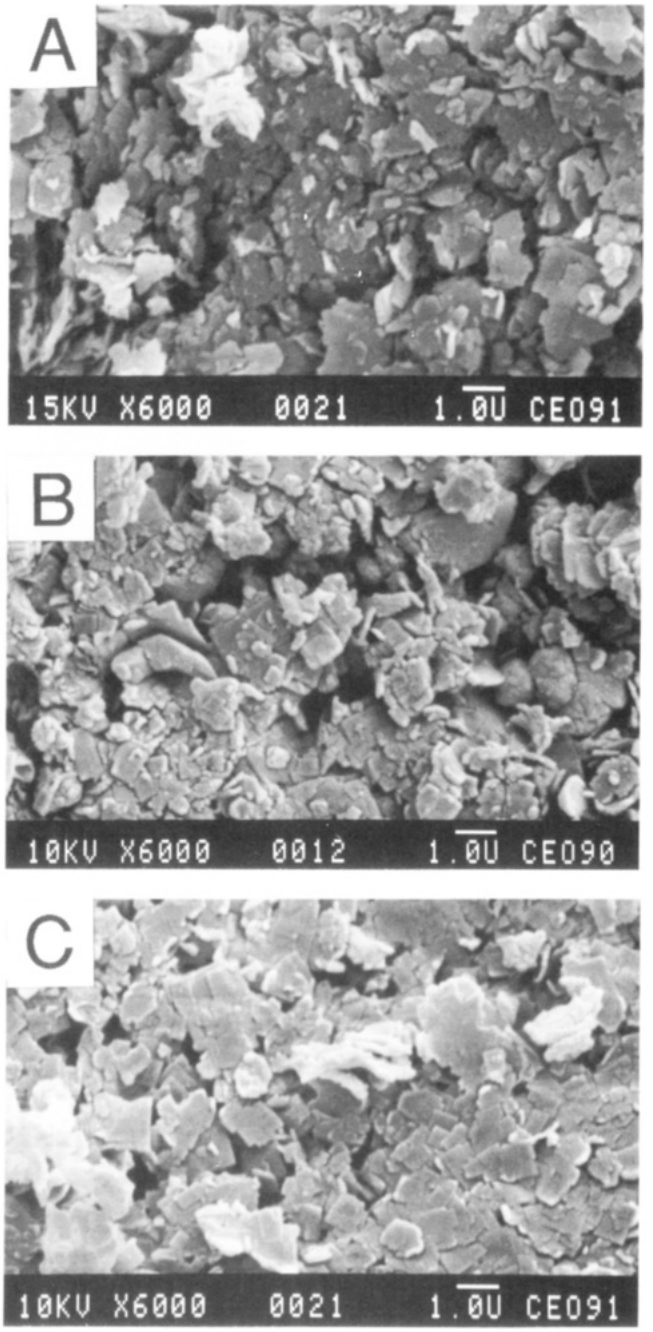

Figure 14. Scanning electron micrographs at ×6000 magnification for (A) air-dried octylammonium–magadiite, (B) TEOS/magadiite reaction product (54:1) air-dried, and (C) calcined TEOS/magadiite (54:1).

intercalate at 360 °C results in the oxidation of octylammonium cations and the formation of hydrated silica pillars in the gallery. The loss of organic matter during the calcination process creates micropores. This reaction sequence is analogous to the general process proposed by Landis et al.[14] for reaction of octylammonium–magadiite with TEOS under related conditions.

The high surface area of the silica-pillared intercalates and their crystallographically regular order along the 001 direction indicate a high degree of uniformity in pillar formation. There are several factors that may contribute to cooperativity in condensation polymerization of TEOS. For instance, the charge density and charge localization of the magadiite layer may help order the space-filling alkylammonium ions in the gallery, and this organization of the ions may be the dominant factor in mediating the final pore structure. Interactions between the ordered

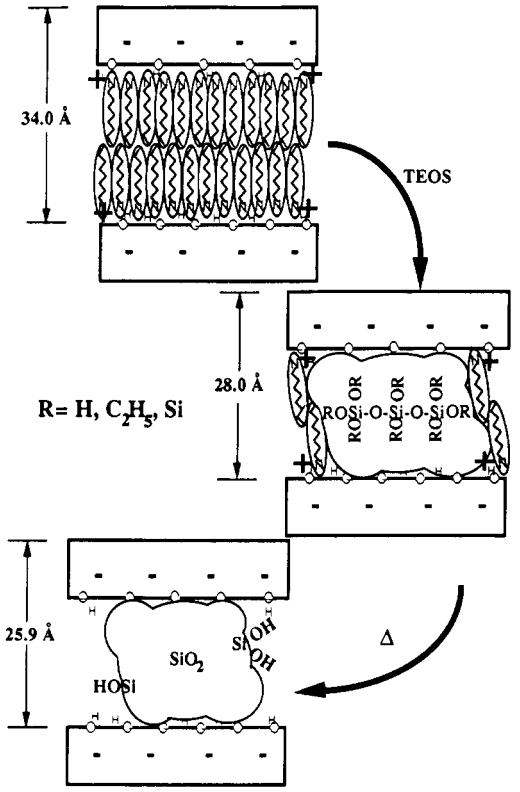

Figure 15. Schematic representation of the pillaring of octylamine solvated octylammonium–magadiite by reaction with TEOS.

alkyl chains of the onium cations also may affect the gallery height. Domains of SiOH groups on the gallery surfaces may function as the initial reaction sites for grafting to TEOS and this could promote topochemical condensation polymerization. A corrugated silicate layer structure containing six-, five-, or four-rings of oxygen also may help control the distribution of onium ions and regulate TEOS polymerization.

Summary and Conclusions

The reaction of H^+–magadiite with octylamine results in a gel-like octylammonium intercalate swollen by neutral octylamine. The fully solvated gel-like derivative has a bilayer structure with a basal spacing of 34 Å, but the basal spacing collapses to 14 Å upon desorption of neutral octylamine. Reaction of the solvated octylamine/octylammonium magadiite gel with TEOS in air results in the intercalation, hydrolysis, and condensation polymerization of TEOS in the magadiite galleries. The condensation is molecularly regular. Polymerization may occur by a topochemical process with the magadiite galleries possibly acting as a template. The final reaction products, after calcination at 360 °C, are composed of layers of magadiite separated by regularly spaced silica pillars. The gallery heights (9.5–14.7 Å) were found to increase with increasing TEOS concentration. However, the microporous surface area (480–670 m^2/g) reached a maximum and then decreased with increasing TEOS concentration. The decrease in surface area with increasing gallery height is attributed to a decrease in the lateral separation of the pillars. Interior surface silanol groups of the type Q^3 $HOSi(OSi)_3$ and Q^2 $(HO)_2Si(OSi)_2$ are present in the final pillared products. The existence of Q^2 sites precludes the possibility of the pillars being precisely isostructural with the magadiite layers.

Finally, we note that the silica pillared magadiite recently reported by Landis et al.[14] was obtained by reaction of an aqueous suspension of octylammonium–magadiite and TEOS. These workers have also shown that other layered materials, such as titanates and metal dichalcogenides, can be pillared by condensation polymerization of metal alkoxides in the intracrystal space. In the case of silica-pillared magadiite their method of synthesis differed from the procedure used in the present work, and the basal spacing of their product (33 Å) was somewhat larger than the range of values observed here (21–26 Å). However, the reported surface area after calcination at 538 °C (530 m^2/g) was in agreement with the range of surface areas found for our materials. Thus, the product reported by Landis et al. most likely possesses the same structural features as the materials reported here.

Acknowledgment. The support of this research by the National Science Foundation (DMR-89 03579) is gratefully acknowledged. J.S.D. also acknowledges a National Institutes of Health student training stipend under the sponsorship of NIEHS Grant 1P42ES04911-01.

Registry No. $Si(OEt)_4$, 78-10-4.